Journal of
Engineering Sciences
Faculty of Engineering
Assiut University
JES
مجلة
العلوم الهندسية
كلية الهندسة
جامعة أسيوط
journal homepage: http://jesaun.journals.ekb.eg

Effect of Silicate Fume -Based Activating Solution on Mechanical Properties of Fly Ash/Silica Fume Geopolymer Concrete

Received 8 May 2025; Revised 16 July 2025; Accepted 16 July 2025

Yasmin Hefni Abdel Aziz[1]
Abeer El Malky[2]

Keywords
Geopolymer, Geopolymerization, Aluminosilicate, Fly Ash, Silica Fume, Alkaline Solution (NaOH, Na_2SiO_3), N-A-S-H / C-A-S-H gel, Rubber, Scanning electron microscope (SEM), energy dispersive spectroscopy (EDS), Si/Al ratio

Abstract: This study introduces a novel approach by entirely substituting commercial Sodium Silicate (Na_2SiO_3) with silica fume (SF), an industrial by-product, to create economical and eco-friendly GC. Fly ash (FA) was partially substituted with SF at proportions of 20%, 25%, 30%, and 35% of the total binder weight to assess its impact on mechanical performance. The alkaline activator solution was employed at 30%, 35%, and 40% of binder weight, with different SF/NaOH ratios (0.75, 1.5, and 2.0) to enhance the activation process. Treated rubber fibers (0.3% by binder weight) were included to improve ductility. The workability and mechanical properties were assessed using slump, compressive strength, splitting tensile strength, flexural strength, and modulus of elasticity tests. Test results indicated that higher SF replacements diminished workability and strength, with a 25% substitution yielding optimal results. The SF-based activator demonstrated comparable strength to traditional methods, attaining optimal performance at an SF/NaOH ratio of 1.5. The inclusion of rubber fibers enhanced the elastic modulus by 10.8%. Microstructural analysis using SEM and EDX confirmed the formation of a denser matrix with fewer cracks and improved bonding. This research presents a viable alternative to commercial activators and proposes a sustainable GC mix design utilizing industrial by-products, contributing to more eco-friendly construction materials

1. Introduction

Geopolymer concrete (GC) is a novel form of zero-cement concrete created by the alkali activation of aluminosilicate-rich material [1]. Several natural and industrial wastes, comprising fly ash (FA) [2-4], pulverized granulated blast furnace slag [5-6], met kaolin [7], red mud [8], and mining wastes [9], can be used to produce GC. FA is a preferred raw material for the production of GC as a result of its different sustainability benefits [10]. Using FA in GC not only reduces the ecological contamination generated by the cement

[1]Assist. professor, Dept. of Civil. Eng., Modern University for Technology & Information, Egypt. yassmin.hefny@eng.mti.edu.eg
[2]Assist. professor, Dept. of Civil. Eng., Modern University for Technology & Information, Egypt. abeer.elmalky@eng.mti.edu.eg

https://doi.org/ 10.21608/jesaun.2025.383265.1506

production but also repurposes industrial waste from thermal power plants, thereby addressing major FA disposal challenges [11]. Apart from its environmental benefits, FA-based GC offers acceptable mechanical properties [12] and has demonstrated high compressive strengths. FA-based GC also demonstrates notable durability and resistance to elevated temperatures. Pavithra et al. [13] reported that this material achieved a compressive strength ($f_{comp.}$) of 54 MPa following 28 days of curing. The research indicates that the mechanical performance of FA-based GC is generally similar to that of conventional ordinary Portland cement (OPC) concrete [14]. Hassan A. et al. [15] noticed that the elastic modulus (Ec) of GC correlates with its compressive strength and aligns closely with values observed in OPC concrete. Similarly, Verma M. et al. [16] reported that, although GC typically exhibits a slightly lower Ec, its remaining mechanical characteristics are satisfactory and broadly equivalent to those of OPC concrete.

"Silica fume (SF), commonly referred to as microsilica or condensed SF, is a by-product generated during the manufacture of silicon or ferrosilicon metals through the reduction of quartz with coal in an electric arc furnace. Recently, there has been increased demand for the use of SF in concrete applications [17]. All grades of silica fume (SF) are applicable in geopolymer technology, presenting a valuable opportunity to reduce accumulated SF waste. Composed primarily of amorphous silicon dioxide (SiO_2 > 90%), SF plays a critical role in enhancing the geopolymerization process, particularly when combined with fly ash (FA). While FA—especially Class F—is rich in aluminosilicate, it generally contains low levels of calcium and reactive silica. Adding SF to the alkaline activator enhances the concentration of reactive silica, which accelerates the dissolution of aluminosilicate species from FA particles. This leads to a higher availability of silicon and aluminium ions for gel formation [18]. As a result, SF supports the development of a denser and more interconnected N-A-S-H (sodium aluminosilicate hydrate) gel structure and, in calcium-rich environments, may also contribute to the development of a hybrid C-A-S-H gel, therefore improving the overall binding strength of the material [19].

Adding SF to GC improves strength, but with optimum values [20, 21]. Chindaprasirt et al. [20] stated that substituting FA with 3.75% SF led to increased strength and durability after 28 days. Correspondingly, Lee et al. [21] found that mixing FA with slag and SF improves the overall reactivity of the GC system. Ergeshov, Örklemez, Ketema et al. 22[21] recently investigated fly ash–based geopolymer mortars containing 2–10% silica fume, assessing their mechanical capabilities, microstructural attributes, and thermal resistance when exposed to temperatures between 300 °C and 900 °C. Their findings suggest that a 2–4% substitution of silica fume yields optimal performance. This is reliable with the findings of Adak, D. et al. [23], who detected the improved mechanical performance when 6% of the FA was replaced with SF. Their results suggest that SF interacts synergistically with FA, contributing to matrix densification and enhancing the bond strength between gel phases. A.N. Sadiq et al. [24] employed response surface methodology to limit the substitution levels of FA and SF for enhancing the mechanical strength of geopolymer mortar. The study examined SF replacement ratios up to 40% and indicated that a composition of 90% FA and 10% SF led to improved mechanical strength.

The majority of studies have utilized FA Class F in the production of GC, as the type of FA significantly influences GC properties. FA is typically classified into low-calcium (Class F) and high-calcium (Class C) categories based on its calcium content. Due to the higher calcium content in the glassy phase, geopolymers made with Class C-FA tend to set more rapidly than those produced with Class F-FA [25, 26]. Calcium facilitates the dissolution of aluminosilicate from FA particles, which progressively increases the concentration of tetrahedral silicate and aluminate monomers in the GC matrix as calcium content rises. This effect corresponds with observed improvements in compressive strength. Additionally, incorporating SF into a low-calcium FA-based geopolymer enhances the microstructure and leads to higher strength development [27]. SF also significantly reduces porosity and permeability [28]. In addition to using SF as a partial replacement material in GC, further investigations have explored its application as a component of the activating solution. Due to its high silicon content and significant early-stage reactivity, SF-resultant activators produce reaction products with properties comparable to those generated by conventional commercial silicate solutions. B. Tempest et al. [29] studied both the result of different curing methods and the performance of NaOH/SF activation systems in comparison to traditional NaOH/Na_2SiO_3 solutions.

The use of an SF-based activating solution caused f_{comp} of approximately 105.1 MPa. Compared to mortars activated with Na_2SiO_3, the addition of SF improved initial and final setting times, flowability, porosity, and shrinkage; however, it resulted in a slight reduction in f_{comp}... Overall, activators formulated with olivine-based nano-SF outperformed those made with commercial Na_2SiO_3, particularly in mixtures with higher SiO_2/Na_2O ratios [30]. The combination of FA and SF solutions as an alternative activator presents a promising research direction, as it not only lowers the energy demand associated with the high-temperature and high-pressure production of Na_2SiO_3 but also maximizes the utilization of SF derived from industrial waste. Although substantial research has been conducted on FA/SF geopolymer blends, limited attention has been given to the use of SF as part of the activating solution rather than solely as a binder component. Most studies rely on conventional alkaline activators such as NaOH and Na_2SiO_3; however, incorporating SF into the activating medium offers the potential for improved control over geopolymer gel formation and matrix densification during early stages of reaction. This gap in the literature represents a significant research deficiency that the current study aims to address.

Geopolymer concrete (GC) generally exhibits lower fracture toughness and tensile strength compared to OPC concrete, leading to more brittle failure modes [31]. This brittleness can be mitigated through the incorporation of various fibbers such as steel, polyvinyl alcohol, sweet sorghum, or cotton. The addition of rubber particles to GC addresses mechanical performance and offers environmental benefits by reducing rubber waste, which is a significant pollutant due to its non-biodegradable nature and accumulation in landfills [31]. However, incorporating rubber into GC tends to reduce its mechanical strength. This decrease is mainly due to the inadequate bonding among the rubber particles and the geopolymer binder [32]. Joker et al. [33] demonstrated that surface treatment of rubber particles with a 1M NaOH solution enhances the adhesion between the rubber and the binder matrix.

2. Research significance

This study introduces a novel, sustainable approach to geopolymer concrete (GC) production by air-curing and enhancing its mechanical properties through the substitution of silica fume (SF) in both binder and activator solution. The SF served two distinct roles: (1) as a partial substitute for fly ash at replacement levels of up to 35% and (2) as an element of the alkaline activator solution, substituting for commercial sodium silicate (Na_2SiO_3). The research explores and compares both approaches to assess the effectiveness of SF in improving GC performance. Treated rubber fibbers were integrated into GC mixtures to enhance ductility. The research methodically investigates various critical factors, encompassing the SF-to-binder ratio, the alkaline solution-to-binder ratio, the Na_2SiO_3-to-NaOH ratio, the effect of utilizing SF as an activator, and the ideal rubber fibber content. This research advances the creation of eco-friendlier and mechanically resilient geopolymer concrete by advocating for the incorporation of industrial by-products in the binder and activator systems.

3. Experimental study

The prime aim of the experimental study is to examine the effects of partially substituting high-calcium FA with SF. The substitution ratios were 20%, 25%, 30%, and 35% of the total binder weight. The overall binder weight in this study was 450 kg/m³. The AL solution's solid components were Na_2SiO_3 and NaOH in a 1:1 ratio. A preliminary study was performed to determine the dose of AL solution, which included two additional binder ratios: 30% and 40%. To explore the effect of mixing ratios of the alkaline solution's solid components, silicate fume and NaOH ratios were further adjusted to 0.75%, 1.5%, and 2.0%. Fig. 1 illustrates the flowchart methodology for determining the optimum components of GC.

3.1 Materials

Fly ash: The used FA is categorized as type C-FA in compliance with ASTM C618-19 [34]. FA has a specific gravity of 2.0 and less than 10% retention on a sieve of 45 microns. The chemical composition and ASTM C618-19 specification requirements are illustrated in Table 1.

Silica fume: It is a light grey by residual material from the ferrosilicon alloys industry. The specific surface area was 16700 m²/kg, and the specific gravity was 2.2. The constituent oxide elements ($SiO_2 + Al_2O_3 + Fe_2O_3$) were 94.6, and the loss of ignition value was 2.0%.

Table 1 shows that the fly ash (FA) meets ASTM C618-19 requirements, with a combined SiO_2, Fe_2O_3, and Al_2O_3 content of 62.8%, indicating good pozzolanic activity. Its high CaO content (24.1%) suggests partial Class C characteristics, enhancing early strength. Silica fume (SF) contains 89% SiO_2, confirming its role as a highly reactive silicate source. Both materials are chemically suitable for geopolymer production, with FA supplying aluminosilicate and SF enhancing matrix densification.

Table 1: Chemical composition of FA and SF (%)

Item%	SiO_2,	Fe_2O_3	AL_2O_3	K_2O	CaO	MgO	Na_2O	L.O.I.
Fly Ash	40.6	4.7	17.5	0.5	24.1	9.4	1.1	1.6
ASTM C618-19[41]	(SiO_2+ Fe_2O_3+ AL_2O_3) >50.0			-	>18.0	-	-	<6.0
Silica Fume	89.0	4.0	1.6	2.2	0.5	0.9	-	2.0

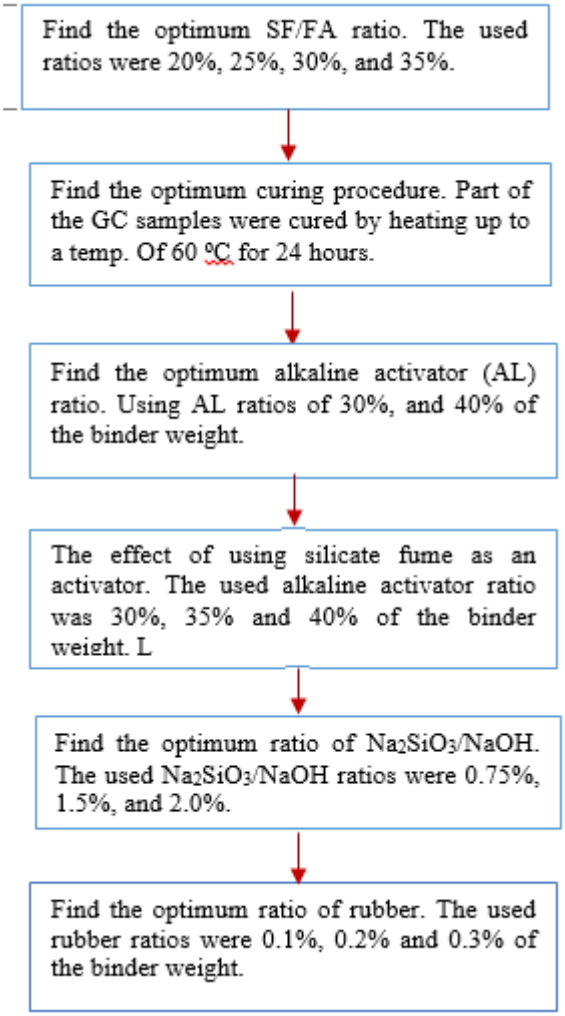

Fig. 1: Flowchart methodology for the study

Alkali activators: FA was activated using alkali-activated solutions prepared by two methods. During the first method, the alkali-activated solution was a mix of two materials: Na_2SiO_3 solution and NaOH solution. A Na_2SiO_3 solution was prepared by dissolving the silica under pressure with an intensive caustic soda solution in the wet procedure, which produces Na_2SiO_3 directly in the solution. Na_2SiO_3 contained 14.7 percent Na_2O and a percentage of 29.4 SiO_2 (SiO_2/Na_2O = 2.00), while the density of the activator was 1.5 g/cm³. A NaOH solution with a molarity of 16 was formulated based on earlier studies [35] through the dissolution of NaOH pellets of 97% purity in deionized water (640 grams are dispersed in 1 liter of water). The NaOH solution was prepared a day before it was mixed with Na_2SiO_3 to ensure cooling.

In the second activation method, Na_2SiO_3 was entirely substituted with silica fume (SF) powder. The SF was incorporated into the NaOH solution. Initially, NaOH flakes were

dissolved in tap water with continuous stirring for three minutes. Subsequently, the SF powder was added to the solution, which was then stirred for an additional five minutes to promote homogeneity. The resulting activating solution was placed in an oven and heated overnight at 75 °C to ensure complete dissolution and interaction between NaOH and SF. Prior to use, the solution was allowed to cool and was maintained at ambient temperature for 24 hours.

Aggregate: Natural siliceous sand with a fineness modulus of 2.85 was employed as the fine aggregate. Crushed dolomite was utilized as coarse aggregate, which complies with the requirement of ASTM C33-07 [36] with a specific gravity of 2.65 and a fineness modulus of 7.87. The size of dolomite particles ranges from 5 to 20 mm.

Rubber fibers: The rubber was collected from waste tires and then prepared manually by cutting it into the required dimensions. The rubber's diameter (D) and length (L) were approximately 2 and 20 mm, respectively; the aspect ratio (L/D) was 10. Rubber's specific gravity was found to be 1.1. The surface of the rubber fibers was chemically treated to increase the adhesion between the GC paste and the rubber surface. The rubber fibers were treated by immersion in a 1-molar NaOH solution for 24 hours [33]. Laterally, particles were extensively rinsed with water multiple times. The rubber particles that had been treated were then allowed to air dry. Figure 2 depicts the used rubber fibers in GC mixes and all of the gradients utilized in the GC mixes.

Fig. 2: The used materials in GC mixes.

3.2. Mix proportions

The parameters of this study were the curing regime, ratios of SF as a partial replacement of FA, ratios of alkaline solution to the binder weight, ratios of Na_2SiO_3 to NaOH activators, the effect of using SF as a silicate activator, and the optimum ratio of rubber fibers to enhance the ductility. To investigate these parameters, 16 concrete mixes were performed. For all mixes, the total binder weight was constant and equaled 450 kg/m³. There isn't a unique mix design method for GCs. The coarse and fine aggregates were used as 75–80% of the total mass in the design of the GC mix for this experiment, which is like OPC concrete. The density of wet GC is taken as 2528 kg/m³ [37]. Solid particles in the Na_2SiO_3 solution account for 50.32% of the entire solution, and water accounts for 49.68%. Fine aggregate accounts for 35% of the total aggregate. The total ratio of water taken is 0.25 of the binder weights [37]. A superplasticizer (SP) was applied to enhance and sustain improved workability for all mixes. Table 2 shows the mix design ratios for different mixes.

Five mixes were prepared to evaluate the effect of partially substituting FA with SF with ratios of 0%, 20%, 25%, 30%, and 35% by weight. In these mixes, the activation alkaline solution in the ratio of 35% of the binder was used, along with Na_2SiO_3 and NaOH solutions

in a ratio of 1:1. Other AL solution ratios of 30% and 40% were examined in two GC mixtures to guarantee the proper use of the AL solution ratio. To explore the effect of using a silicate fume-based activating solution, three mixtures were used by completely substituting Na_2SiO_3 with SF and using an AL solution with ratios of 30%, 35%, and 40%. Laterally, three mixes were used to investigate the impact of the activator component ratio (silicate fume/NaOH) on the mechanical properties of GC; the silicate fume and NaOH ratios were adjusted to 0.75%, 1.5%, and 2.0%, respectively. Finally, three mixtures were prepared to investigate the effect of adding rubber in ratios of 0.1, 0.2, and 0.3% based on the total binder material.

Table 2: Mix proportions (kg/m^3)

Mix ID	FA	SF	Silicate powder	NaOH	Na_2SiO_3	AL ratio	Water in solution	Excess water	Sand	Coarse Agg.	Rubber	Si/Al ratio
FA 450-A0.35	450.0	-	-	78.75	78.75	0.35	87.6	23.2	664	1,233	-	2.85
SF 0.20-A0.35	360.0	90.0	-	78.75	78.75	0.35	87.6	23.2	664	1,233	-	3.98
SF 0.25-A0.35	337.5	112.5	-	78.75	78.75	0.35	87.6	23.2	664	1,233	-	4.43
SF 0.30-A0.35	315.0	135.0	-	78.75	78.75	0.35	87.6	23.2	664	1,233	-	4.67
SF 0.35-A0.35	292.5	157.5	-	78.75	78.75	0.35	87.6	23.2	664	1,233	-	5.5
SF 0.25-A0.30	337.5	112.5	-	67.50	67.50	0.30	75.0	35.8	668	1,240	-	4.29
NSF 0.25-A0.30	337.5	112.5	34.0	67.50	-	0.30	41.5	69.3	668	1,240	-	4.29
SF 0.25-A0.40	337.5	112.5	-	90.00	90.00	0.40	100.1	10.8	661	1,227	-	4.5
NSF 0.25-A0.40	337.5	112.5	45.3	90.00	-	0.40	55.4	55.5	661	1,227	-	4.5
NSF 0.25-A0.35	337.5	112.5	39.6	78.75	-	0.35	46.8	64.0	664	1,233	-	4.43
SN0.75	337.5	112.5	34.0	90.00	-	0.35	55.4	55.5	665	1,234	-	4.29
SN1.5	337.5	112.5	47.6	63.00	-	0.35	38.7	72.1	663	1,232	-	4.53
SN2.0	337.5	112.5	52.8	52.50	-	0.35	32.3	78.5	663	1,231	-	4.59
SF 025-R 0.10	337.5	112.5	39.6	78.75	-	0.35	46.8	64.0	664	1,233	4.5	4.43
SF 0.25-R 0.20	337.5	112.5	39.6	78.75	-	0.35	46.8	64.0	664	1,233	9.0	4.43
SF 0.25- R 0.30	337.5	112.5	39.6	78.75	-	0.35	46.8	64.0	664	1,233	13.5	4.43

Table 2 presents detailed mix proportions for various GC formulations. The reference mix (FA 450-A0.35) used 450 kg/m³ of FA without SF or rubber. Increasing SF substitution (from 20% to 35%) elevated the Si/Al ratio (from 3.98 to 5.5), enhancing mix reactivity. AL ratios ranged from 0.30 to 0.40 to evaluate activator content influence. Substitution of Na_2SiO_3 with silica fume powder (NSF series) maintained the Si/Al ratio while increasing excess water. Rubberized mixes (R series) had constant binder content but increasing rubber proportions (0.10–0.30) to assess ductility effects. Overall, the table enables a comprehensive comparison of mix design parameters influencing the strength, workability, and durability of geopolymer concrete.

3.3. Mixing and casting

The laboratory manufacturing procedure for GC mixtures is illustrated in Fig. 3. Aggregates were fed into the drum mixer, then FA and SF were added and mixed for five minutes. Then, the activating solutions and the calculated excess water were gradually added and mixed for five minutes. Finally, rubber fibers were added to the mix. To make concrete workable, superplasticizer is added to GC mixes, and the dosages are adjusted to achieve

acceptable workability. The testing samples were cast. Thereafter, all of the samples were vibrated for two minutes.

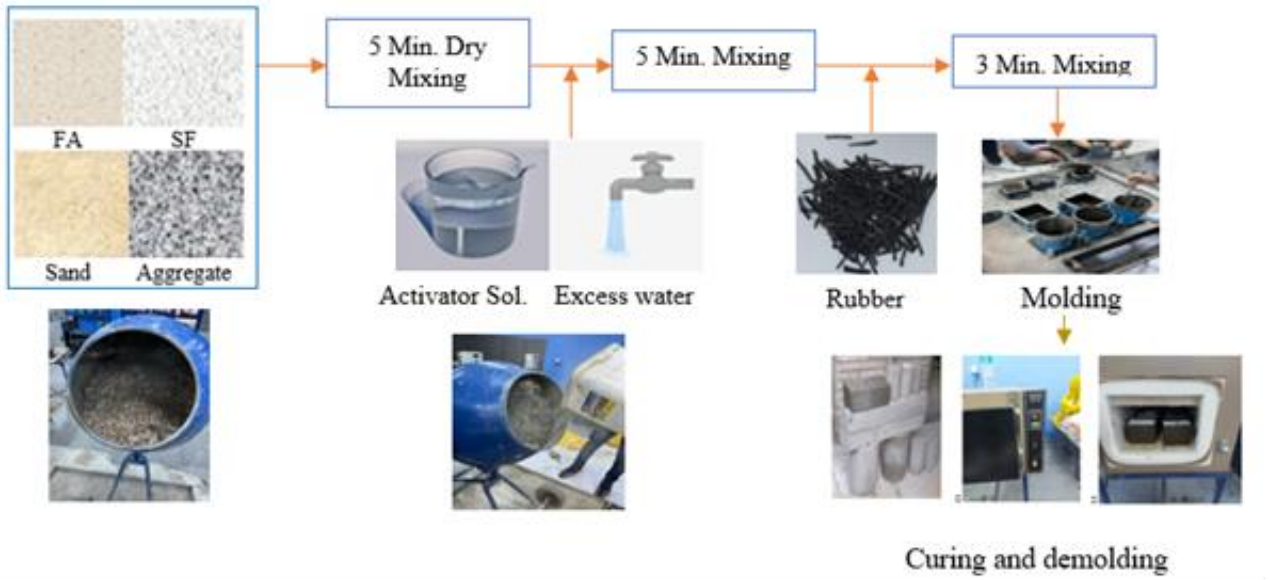

Fig. 3: Preparation process chart.

3.4. Test procedures

The intended slump of concrete was 100 mm. The $f_{comp.}$ was determined using cubic samples 100 x 100 x 100 mm prepared as per EN 12390 3:2002 [38], and the tensile strength ($f_{ten.}$) was determined using cylinders 100 x 200 mm prepared as per ASTM C 496-90 [39]. Prisms of 100 x 100 x 500 mm were used to measure the flexural strength (f_{flex}). In compliance with ASTM C 78-02 [40]. The modulus of elasticity (Ec) was determined using cylinders 150 x 300 mm according to ASTM 469 -02 [41]. All samples were kept in molds for 24 hours at room temperature. After demolding, GC samples were left in the air at ambient temperature (25°C) until testing. Test set up for assessing the mechanical properties is presented in Fig. 4.

Compressive strength | Splitting tensile strength | Flexural strength | Modulus of elasticity

Fig. 4: Test setup for assessing the mechanical properties

To explore the efficiency of GC air curing, part of the GC samples–mixes FA 450-A0.35, SF 0.20-A0.35, SF 0.25-A0.35, SF 0.30-A0.35, and SF 0.35-A0.30 – were cured by heating up to a constant temperature of 60°C for 24 hours; this temperature was chosen according to the previous studies [42]. In these studies, the authors found that GC samples cured at 60°C

for 24 hours exhibited greater strength compared to those cured at other heating temperatures and durations.

4. Results and discussion

The mixture containing 100% FA exhibited the highest slump value of 120 mm, indicating excellent workability. However, workability decreased markedly with the partial replacement of FA by SF. Slump values corresponding to 25% and 35% SF substitution were recorded at 100 mm and 80 mm, respectively. The mix with 35% SF exhibited rapid setting and hardening, which hindered proper molding of the specimens. This reduction in workability is likely attributed to the high surface area of SF. These results suggest that incorporating SF into FA-based geopolymer concrete significantly diminishes workability. Nonetheless, despite the decline, the workability remained within acceptable limits, as the concrete maintained a plastic consistency, confirmed by a compaction factor of 0.9. The slump value for the SF 0.25–R 0.30 mix was comparatively low (60 mm), which was expected due to the irregular shape of the rubber particles used. Consequently, the superplasticizer content was gradually increased in the GC mixes to achieve the target slump value of 100 mm. Figure 5 illustrates the results of the slump tests.

FA 450-A0.35 SF 0.25- R 0.30

Fig.5: Slump test

4.2 Effect of curing regime on strength

Extensive research has indicated the importance of heat curing in enhancing the performance of GC. However, the reliance on elevated-temperature curing is often considered a limitation to the broader application of FA-based GC in conventional cast-in-place construction. Despite growing interest, limited data is available on the structural viability of GC mixtures cured under ambient conditions. Therefore, it is essential to examine the behaviour of GC cured without heat, particularly when SF is used to partially replace FA. In this study, selected GC specimens underwent thermal curing at a consistent temperature of 60 °C for 24 hours, while others were subjected to ambient air curing. The compressive strength values for both curing methods, evaluated at 3, 7, and 28 days, are presented in Table 3.

According to the results presented in Table 3, the heat-cured specimens of mix FA 450-A0.35 (containing 0% silica fume) exhibited higher compressive strengths by 79.0%, 23.0%, and 2.0% at 3, 7, and 28 days, respectively, compared to their air-cured counterparts.

For the mix containing 25% SF (SF 0.25-A0.35), the corresponding strength increases due to heat curing were 75.0%, 19.8%, and 0.01%, while for the mix with 35% SF (SF 0.35-A0.35), the gains were 68.1%, 19.8%, and 0.00% at the same respective ages. These findings suggest that by 7 and 28 days, air curing provided comparable strength development to heat curing across all mix compositions.

Table 3: Compressive strength of GC samples under heat exposure and air curing (N/mm^2)

Mix ID	Heat Curing			Air Curing		
	3	7	28	3	7	28
FA 450-A0.35	37.2	41.3	47.2	20.7	33.5	46.3
SF 0.20-A0.35	37.2	40.6	43.0	21.0	33.3	43.0
SF 0.25-A0.35	36.9	39.3	42.1	21.0	32.8	41.7
SF 0.30-A0.35	31.0	33.0	37.3	18.2	27.2	35.7
SF 0.35-A0.35	30.0	31.0	34.0	17.8	25.9	33.9

As shown in Table 3, the incorporation of Class C fly ash as the primary binder contributed to improved compressive strength under ambient curing conditions across all mixes. This behaviour is attributed to the high calcium content in FA Type C, which enables strength development without the need for elevated temperatures. The formation of a crystalline calcium silicate hydrate (C–S–H) phase at higher calcium levels facilitates hardening even under air curing [43]. Although increasing the SF content led to a reduction in compressive strength at 28 days, mixes containing up to 25% SF retained or slightly enhanced their early-age strength (at 3 and 7 days). This may be attributed to the formation of a denser microstructure [44]. The ultra-fine particles of silica fume act as micro-fillers through a packing mechanism, dispersing uniformly within the geopolymer matrix and filling voids in the GC paste microstructure [45].

4.3 Impact of partial substitution of FA with SF on strength

To assess the effect of SF substitution on the strength development of GC, five substitution levels were examined: 0%, 20%, 25%, 30%, and 35%. All mixtures were prepared using a constant alkaline solution-to-binder ratio (A/L) of 0.35 and a fixed Na_2SiO_3/NaOH ratio of 1.0. The outcomes of $f_{comp.}$ $f_{ten.}$, $f_{flex.}$ Tests conducted at 7 and 28 days are presented in Figures 6, 7, and 8, respectively.

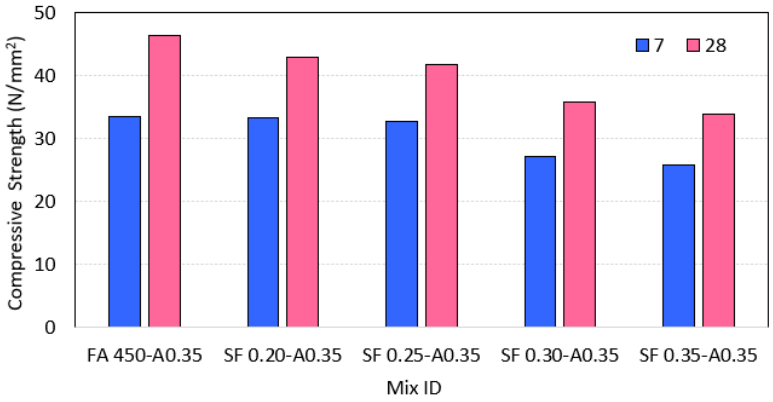

Fig. 6: Compressive strength (N/mm^2)

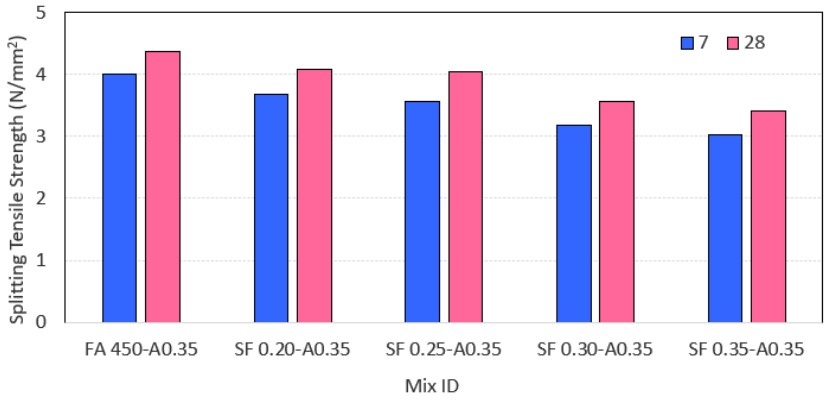

Fig. 7: Splitting tensile strength (N/mm^2)

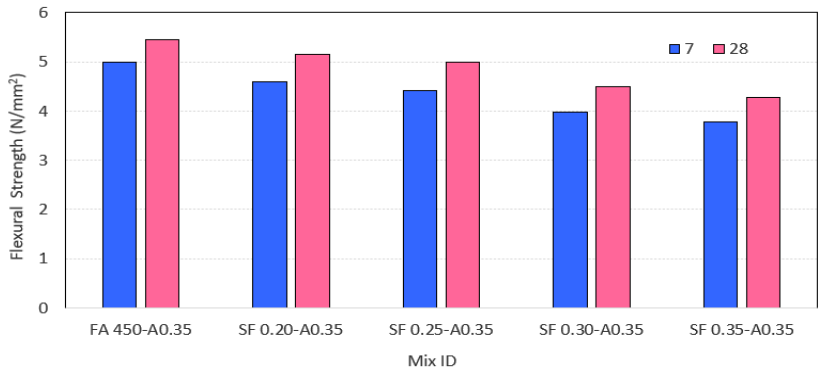

Fig. 8: Flexural strength (N/mm^2)

Referring to the GC mixes in the above figures, it is obvious that GC strengths were reduced by increasing the SF substitution ratio. At the SF 0.20-A0.35 mix, the $f_{comp.}$ Was reduced by 7.1% at 28 days when compared with FA 450-0.35. Similar trends were observed for tensile and flexural strengths. They were reduced by 6.3% and 5.5%, respectively. When increasing the replacement ratio to 25%, the corresponding reduction was increased to 9.9%, 7.9%, and 8.4%, respectively. Over the 25% substitution ratio, a sharp reduction in strength was observed. At the SF 0.30-A0.35 mix, the $f_{comp.}$ $f_{ten.}$, f_{flex} were reduced by 22.9%, 18.4%, and 17.6%, respectively.

Based on the results illustrated in the aforementioned figures, it is evident that increasing the SF substitution ratio led to a reduction in the mechanical strengths of the GC mixes. For the SF 0.20–A0.35 mix, the compressive strength at 28 days decreased by 7.1% compared to the control mix (FA 450–A0.35). Similar decreasing trends were recorded for the splitting tensile and flexural strengths, which declined by 6.3% and 5.5%, respectively. When the SF replacement ratio was increased to 25%, the corresponding reductions in compressive, tensile, and flexural strengths rose to 9.9%, 7.9%, and 8.4%, respectively. Beyond the 25% substitution level, the decline in strength became significantly more pronounced. At the SF 0.30–A0.35 mix, reductions of 22.9%, 18.4%, and 17.6% were observed for $f_{comp.}$ $f_{ten.}$, f_{flex}, respectively.

According to the findings, the replacement ratio of 25% was the most beneficial. GC preserves 90% of its $f_{comp.}$ At this proportion compared to FA 450-0.35, so with only 5% additional SF substitution in the SF 0.30-A0.35 mix, the ratio is reduced to 77.1%. The high

strength reduction was obviously guaranteed at mix SF 0.35–A0.35. The $f_{comp.}$ $f_{ten.}$, and $f_{flex.}$ Were reduced by 26.7%, 21.8%, and 21.7%, respectively. Based on these results, the SF substitution ratio of 25% was then employed in all research mixtures.

The observed reduction in strength with increasing SF content can be attributed to the extremely fine, spherical nature of SF particles. At lower substitution levels, these particles contribute to a denser and more compact microstructure by effectively filling internal voids. However, beyond a certain threshold, the excess SF tends to agglomerate within localized regions, disrupting the matrix continuity and leading to strength deterioration [46]. To mitigate the negative impact of silica congestion, it is essential to optimize the SF dosage and maintain an appropriate balance with the alkaline activators to preserve the geopolymer concrete's reactivity and mechanical performance. In this study, SF was directly mixed with the alkaline solution to form the activated slurry [47].

4.4 Effect of AL ratios on strength

At this stage of the investigation, A/L ratios of 0.30, 0.35, and 0.40 were examined, with the SF substitution ratio fixed at 25%. The ratios of Na_2SiO_3/NaOH and SF/NaOH were maintained at 1.0 across all mixes. The total water content was kept constant at 112.5 kg/m³ in each mixture. Figures 9, 10, and 11 present the $f_{comp.}$ $f_{ten.}$, f_{flex} results, respectively, for evaluating the influence of the A/L ratio at 7 and 28 days.

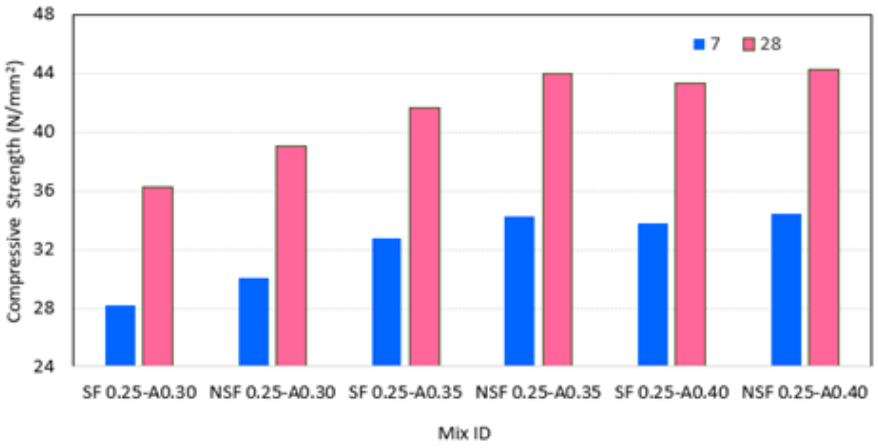

Fig. 9: Compressive strength for the effect of AL ratio (N/mm^2)

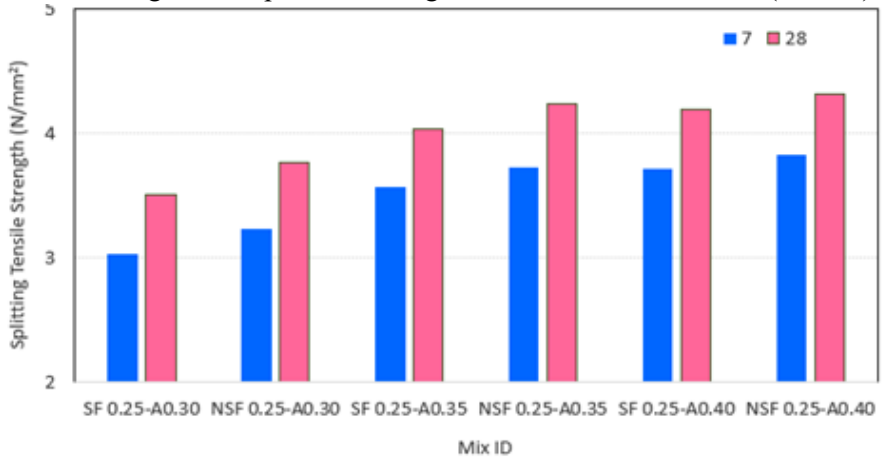

Fig. 10: Splitting tensile strength for the effect of AL ratio (N/mm^2)

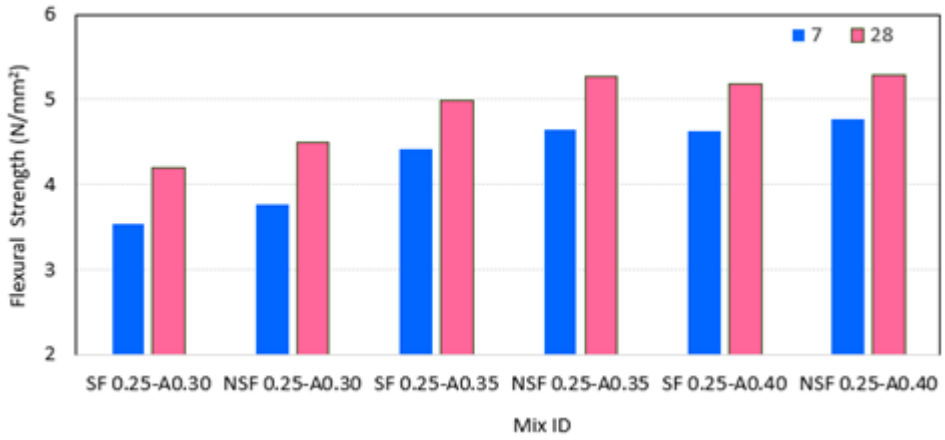

Fig. 11: Flexural strength for the effect of AL ratio (N/mm2)

At 7 days, the $f_{comp.}$ Of mixes SF 0.25–0.30 and SF 0.25–0.35—corresponding to A/L ratios of 0.30 and 0.35—increased from 28.2 MPa to 32.8 MPa. Further increasing the A/L ratio to 0.40 resulted in an $f_{comp.}$ Of 33.80 MPa. This enhancement continued through to 28 days, with $f_{comp.}$ Rising from 36.30 MPa to 41.70 MPa as the A/L ratio increased from 0.30 to 0.35. A further increase in the A/L ratio from 0.35 to 0.40 led to a modest strength gain, reaching 43.49 MPa at 28 days. These findings demonstrate that increasing AL from 0.35 to 0.40 exhibits a lower strength development rate than increasing AL from 0.30 to 0.40. Similar trends have been observed for splitting and flexural strength.

The geopolymerization process is often separated into two steps: dissolution-hydrolysis and hydrolysis-polycondensation. When the AL ratio increases, silicon species, sodium ions, and base water increase. All of these variables influence the geopolymerization process and strength. At the dissolution-hydrolysis step, SiO_2 and Al_2O_3 species occur [48]. Increasing silicon species formed more Si-O-Si bonds and increased the SiO_2/Al_2O_3 ratio, which improved geopolymer strength [49]. Base water plays a critical role in the geopolymerization process, as highlighted by previous studies [49]. An increase in base water content facilitates the enhanced dissolution of SiO_2 and Al_2O_3 species, thereby generating a greater concentration of hydrolysed ions during the second stage of the reaction. This leads to an accelerated geopolymerization rate, ultimately contributing to the development of a higher-strength geopolymer matrix.

4.5 Effect of using silicate fume as an activator on strength

To evaluate the effect of using silicate fume as an activator, a portion of SF is mixed with NaOH solution; the weight of SF is equal to the solids in the Na_2SiO_3 activator. The activator ratios used were 0.30, 0.35, and 0.40, whereas the Na_2SiO_3/NaOH ratio remained constant at 1.0. The mix proportions for these geopolymer mixes are detailed in Table 2. The study evaluated the $f_{comp.}$ $f_{ten.}$, and $f_{flex.}$ Of the resulting geopolymer specimens at ages 7 and 28 days, and the outcomes are displayed in Figs. 12, 13, and 14. As illustrated in Figs. 12, 13, and 14, substituting silicate fume (SF) as an activator instead of Na_2SiO_3 in geopolymer mixes with AL ratios of 0.30, 0.35, and 0.40 (mixes NSF 0.25-0.30, NSF 0.25-0.35, and NSF 0.25-0.40) led to slight enhancements in compressive strength at 28 days.

These enhancement ratios were 7.5%, 5.5%, and 2.0%, respectively. Splitting and flexural strength showed similar trends.

Referring to the above results, the strength results for all mixes after using silicate fume activators are comparable with those after using Na_2SiO_3 activators. The silica fume-based activators produce reaction products closely resembling those formed with sodium silicate, owing to the high reactivity of silica fume, which supplies a significant amount of soluble silica from the early stages of geopolymerization [50]. As a result, it has been demonstrated that using SF as an activator is effective, even with low alkaline ratios in GC mixtures.

The incorporation of Na_2SiO_3 into the NaOH-based activator does not lead to the formation of any new crystalline phases within the geopolymer matrix, but it considerably enhances silicate and aluminate dissolution from the source material [51]. Soluble silicate species in Na_2SiO_3 solution are employed for the condensation of alkali-activated binders [52]. Extra silicates in the solution, on the other hand, impede the structural development of geopolymers [53]. Excess OH in the GC mix is formed by the creation of a two-dimensional network with linearly connected polymeric structures [54]. This results in a decline in its characteristics [1]. In contrast, NaOH has typically been used to dissolve Si^{4+} and Al^{3+} ions from FA in order to produce aluminosilicate materials. NaOH exhibits a superior ability to liberate silicate and aluminate monomers due to its stronger zeolitization capacity, and sodium cations are more crucial for the creation of the GC structure [55]. On the other hand, other scientists argued that a higher salt concentration would lead to the production of sodium carbonate through air carbonation, which would obstruct the polymerization process and reduce compressive strength [56]. To investigate the impact of the silicate fume/NaOH ratio on GC strength, Mix NSF 0.25-0.35 was chosen as a reference. In this mix, the silicate fume/NaOH ratio equals 1.0. Three other silicate fume/NaOH ratios of 0.75, 1.5, and 2.0 were compared. The AL ratio examined in these mixes was 0.35. The output of tests for $f_{comp.}$, $f_{ten.}$, f_{flex} at ages 7 and 28 days is displayed in Figs. 12, 13, and 14.

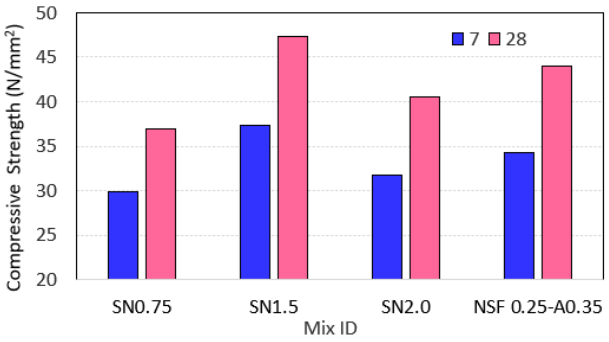

Fig. 12: Compressive strength for the impact of silicate fume /NaOH Ratio (N/mm^2)

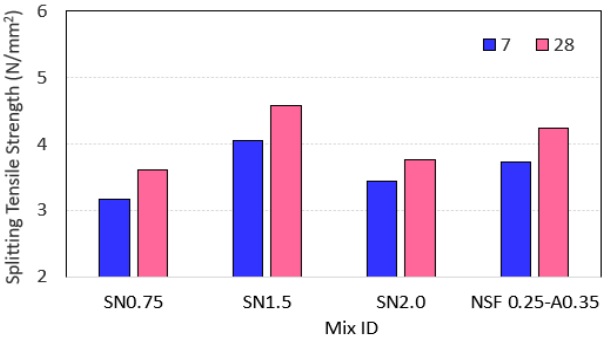

Fig. 13: Splitting tensile strength for the impact of silicate fume /NaOH Ratio (N/mm^2)

The results illustrated in the figures indicate that increasing the silicate fume/NaOH ratio led to an improvement in the mechanical properties of GC up to an optimal ratio of 1.5. Beyond this value, a decline in strength was observed. Specifically, increasing the silicate fume/NaOH ratio from 0.75 to 1.0 resulted in enhancements of 19.1%, 17.2%, and 22.0% in compressive, tensile, and flexural strengths at 28 days, respectively. Further increasing the

ratio to 1.5 led to maximum strength gains of 28.0% for $f_{comp.}$ 26.9% for $f_{ten.}$, and 29.8% for f_{flex}.

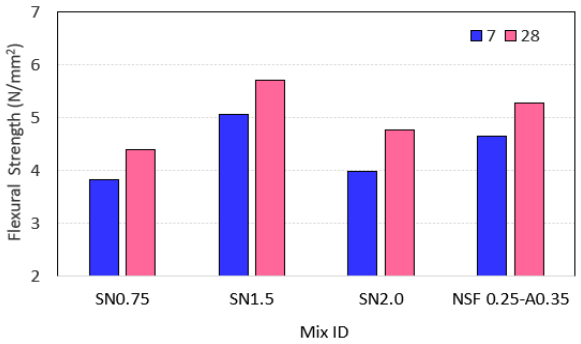

Fig. 14: Flexural strength for the impact of silicate fume /NaOH Ratio (N/mm^2)

The enhancement in the intensity of GC is due to the elevated concentration of soluble silicate in the activator solution. Soluble silicates facilitate geopolymer polycondensation [57]. Nonetheless, elevated concentrations of soluble Na_2SiO_3 impede the geopolymerization process. This is due to the inclusion of additional silicates in the mixture, which impede the formation of geopolymeric structures, leading to a reduction in strength [56]. The strength drop may be attributed to the Na_2SiO_3/NaOH ratio above 1.5.

It is reasonable to assume that the behavior of silica fume in geopolymer concrete (GC) is comparable to that of Na_2SiO_3, given their similar chemical contributions. The observed strength enhancement can be linked to the intricate nature of the geopolymerization process. One plausible explanation for this improvement is the increase in the Na_2SiO_3/NaOH mass ratio, which leads to a higher availability of SiO_2 species. This, in turn, elevates the SiO_2/Al_2O_3 ratio, promoting the formation of a greater number of Si–O–Si bonds. Since Si–O–Si linkages are stronger than Si–O–Al bonds, the resulting geopolymer matrix exhibits improved mechanical strength.

4.6 Effect of incorporating rubber fibers on strength

Rubber ratios of 0.10, 0.20, and 0.30% were investigated. The AL ratio was 0.35. Silicate fume activator was used. Figs. 15, 16, and 17 show the results of $f_{comp.}$ $f_{ten.}$, and $f_{flex.}$ Tests for concrete mixtures at ages 7 and 28 days.

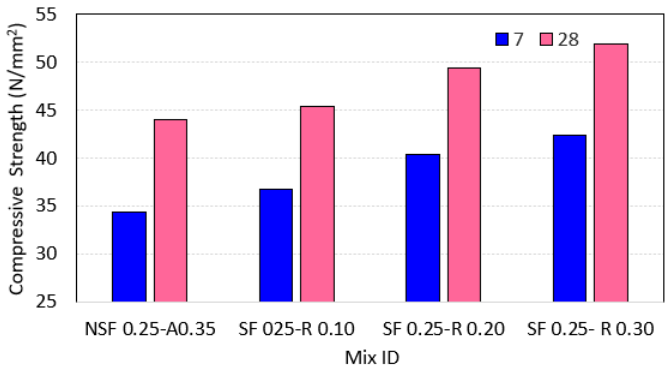

Fig. 15: Compressive strength for the effect of rubber (N/mm^2)

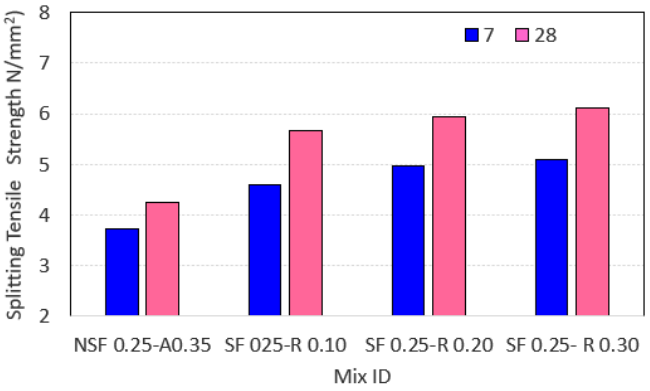

Fig. 16: Splitting tensile strength for the effect of rubber (N/mm^2)

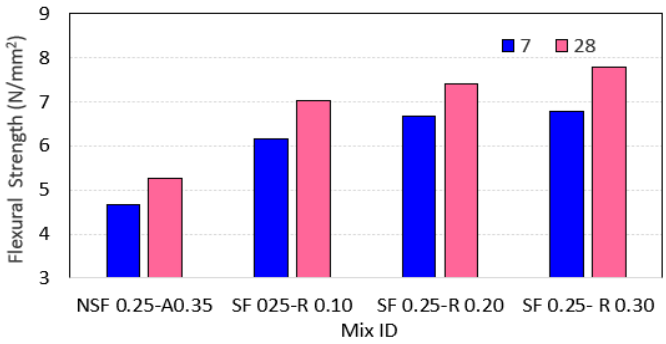

Fig. 17: Flexural strength for the effect of rubber (N/mm^2)

Referring to the above figures, it is obvious that when the proportion of rubber fibers increased, the $f_{comp.}$ Gradually improved. Adding the rubber up to a ratio of 0.30% improved the $f_{comp.}$ $f_{ten.}$, and $f_{flex.}$ At 28 days by 25.7%, 44.5%, and 47.8%, respectively. In fact, adding rubber was expected to improve the splitting and flexural strength and reduce the compressive strength; increasing the $f_{comp.}$ Is owed to the effective treatment process of the rubber surface using NaOH solution, which enhances the bond between the binder and rubber surface. In addition, the rubber was used in a low portion (up to 0.30%).

a. Compression for FA 450-A0.35 samples

b. Compression for SF 0.25-R0.30 samples

c. Splitting for FA 450-A0.35 samples

d. Splitting for SF 0.25-R 0.30 samples

e. Flexural for SF 0.25-R 0.30 samples

Fig. 18: Mode of failure

The failure modes observed during the $f_{comp.}$ $f_{ten.}$, and f_{flex} tests for both FA 450-A0.35 and rubberized specimens (SF 0.25–R 0.30) are presented in Fig. 18. As shown, the failure

patterns are largely comparable across both mixes, suggesting that the inclusion of rubber had a minimal effect on altering the overall mode of failure. However, the slight variations observed indicate a reduction in brittleness and a marginal enhancement in the ductility of the GC due to rubber incorporation.

The effect of rubber inclusion on the modulus of elasticity (Ec) was observed by evaluating GC specimens at 28 days. The assessment was conducted for three mix designs: FA 450-A0.35, NSF 0.25-A0.35, and SF 0.25-R0.30. The Ec values obtained after 28 days are illustrated in Fig. 19.

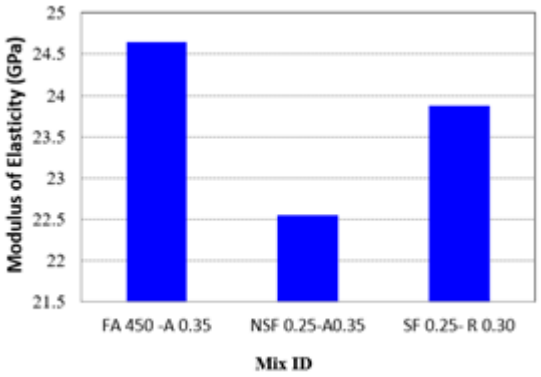

Fig. 19: Modulus of elasticity (Ec) of GC mixes after 28 days of curing.

The modulus of elasticity (Ec) is a key parameter for assessing the structural performance of concrete under service loads. For geopolymer concrete, Ec has been reported to reach approximately 89% of that of OPC concrete with similar $f_{comp.}$, and the stress–strain behavior in compression was similarly aligned when the same aggregate type was used [16]. In a related study, Olivia and Nikraz [58] reported that the Ec of 100% fly ash-based geopolymer concrete was 14.9–28.8% lower than that of the OPC control mix.

Although alkali-activated natural pozzolan mixes exhibited lower Ec values compared to OPC mixtures during the initial 14 days, Bondar et al. [59] reported that, over extended curing periods, the Ec values surpassed those of OPC mixes by approximately 5–20%. Consequently, the Ec of geopolymer concrete (GC) has shown considerable variability across different studies. It is noteworthy that most of these findings were derived from experiments conducted on heat-cured GC specimens.

According to Fig. 19, while the compressive strength of the 0.30% rubber mix SF 0.25-R 0.30 is 25.7% higher than that of the NSF 0.25-A0.35 mix, the elastic modulus increased only by 10.8 with the addition of rubber, indicating that the rubber enhances the ductility of GC. By replacing 25% of FA with SF, the modulus of elasticity was lowered by 12.6%.

Considering the significance of figuring out E_c for evaluating how efficiently a structure performs in service, numerous attempts have been made to develop straightforward formulas that could predict Ec for OPC [60-62] and GC concrete [63]. The applied models include: The American Concrete Institute Committee 318 equation [61]:

$$E_c = 4700 \sqrt{f_{comp.}} \qquad (N/mm^2) \qquad (1)$$

This equation is commonly employed in traditional OPC concrete designs and presumes a robust link between compressive strength and elastic modulus.

$$\text{Iravani [64]: } E_c = 3800 \sqrt{f_{comp.}} \quad (N/mm^2) \tag{2}$$

This model, designed for alternate cementitious materials, reduces the coefficient in relation to ACI to more accurately represent the reduced stiffness typically observed in GC systems.

$$\text{Nath et al. [63]: } E_c = 4100 \sqrt{f_{comp.}} \quad (N/mm^2) \tag{3}$$

This equation is specifically designed for FA-GC, considering the nonlinear stiffness-gain behavior characteristic of GC materials.

$$\text{AS 3600 [62]: } E_c = \rho^{1.5} (0.024 \sqrt{f_{comp.}} + 0.12) \quad (N/mm^2) \tag{4}$$

This Australian standard uniquely incorporates the influence of concrete density, which is especially pertinent for rubberized GC due to its significantly diminished material density.

Where:

E_c: The modulus of elasticity (N/mm^2)

$f_{comp.}$ The compressive strength at 28 days (N/mm^2)

ρ : The density (kg/cm^3)

In this investigation, the values for Ec were predicted based on the above models. The calculated modulus of elasticity values was compared with the corresponding experimental results, as indicated in Table 4.

Table 4: Comparison between experimental and predicted values of modulus of elasticity (Ec) for GC mixes.

Mix ID	$f_{comp.}$ (N/mm^2)	ρ (kg/cm^3)	Exp. E_c (GPa)	ACI [91]	Iravani [86]	Nath et al. [93]	AS 3600]92[
FA 450 -A 0.35	46.29	2120	24.65	31.98	25.85	27.90	27.65
NSF 0.25-A0.35	43.99	2100	22.55	31.17	25.20	27.19	26.89
SF 0.25- R 0.30	51.86	1980	23.88	33.85	27.37	29.53	25.78

ACI 318 [61] substantially overestimated Ec for all GC combinations. The variances were 29.7%, 38.2%, and 41.8%, respectively. This overestimation underscores its restricted application for GC, especially those cured in ambient temperatures, as it was first designed for OPC. Relying on ACI forecasts in structural design could lead to an underestimation of deflections and an overestimation of stiffness. This situation may result in serviceability issues, including inaccurate evaluations of mid-span crack widths in GC elements. Iravani's model [64] had the most accurate correlation with experimental data for the non-rubberized mixtures. The discrepancies were 4.9% for FA 450 - A 0.35 and 11.8% for NSF 0.25 - A 0.35. This statistic signifies its superior precision in depicting the elastic behavior of GC during ambient curing conditions.

The AS 3600 model [62] provided the most precise prediction for the rubberized mix (SF 0.25 - R 0.30), exhibiting a variance of merely 7.96%. The enhanced performance is likely

attributable to the model's incorporation of density (ρ), a crucial element, as the introduction of rubber diminishes density and hence stiffness. AS 3600 is a more appropriate framework for redesigned GC utilizing lightweight or recycled materials. Finally, the equation proposed by Nath et al. [63], although tailored for FA-based GC, yielded moderate overestimations with deviations of 13.2%, 20.6%, and 23.7%, respectively. Although this model surpassed ACI 318, its precision remained inferior to the Iravani and AS 3600 models, particularly for high-strength or changed GC compositions. Consequently, the research emphasizes the necessity of employing mix-specific Ec models for geopolymer concrete. The findings confirm the appropriateness of the Iravani model for conventional GC and the AS 3600 model for rubberized GC, indicating that typical OPC-based models require recalibration for GC systems to provide dependable structural analysis.

5. Microstructural and EDX Spectrum Analysis:

Scanning Electron Microscopy (SEM) and Energy-Dispersive X-ray (EDX) spectroscopy were employed to investigate the microstructural characteristics of FA-based GC at 28 days of curing. Figure 20 displays SEM images for three different mixes: SF 0.25-A0.35, NSF 0.25-A0.35, and SN2.0. The SF 0.25-A0.35 mix was prepared using an NaOH to Na_2SiO_3 ratio of 1:1, while the mixes NSF 0.25-A0.35 and SN2.0 were designed to examine the influence of partially replacing Na_2SiO_3 with silicate fume at substitution levels of 1% and 2.0%, respectively.

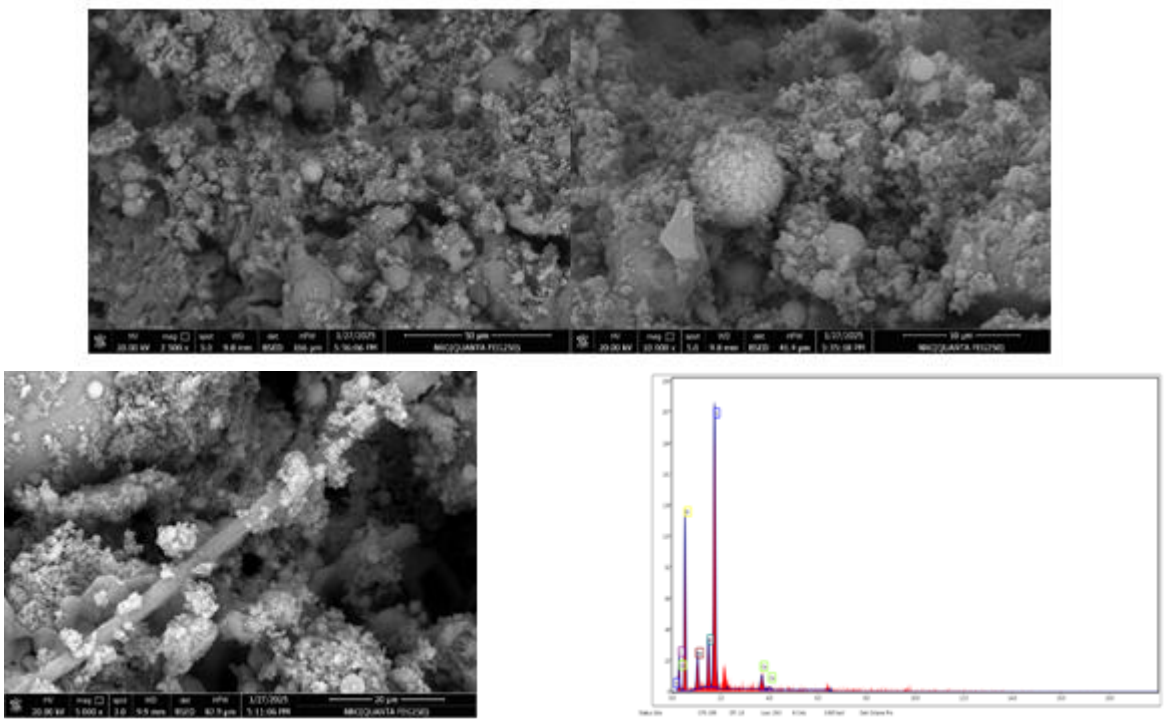

(a) SF 0.25-A0.35

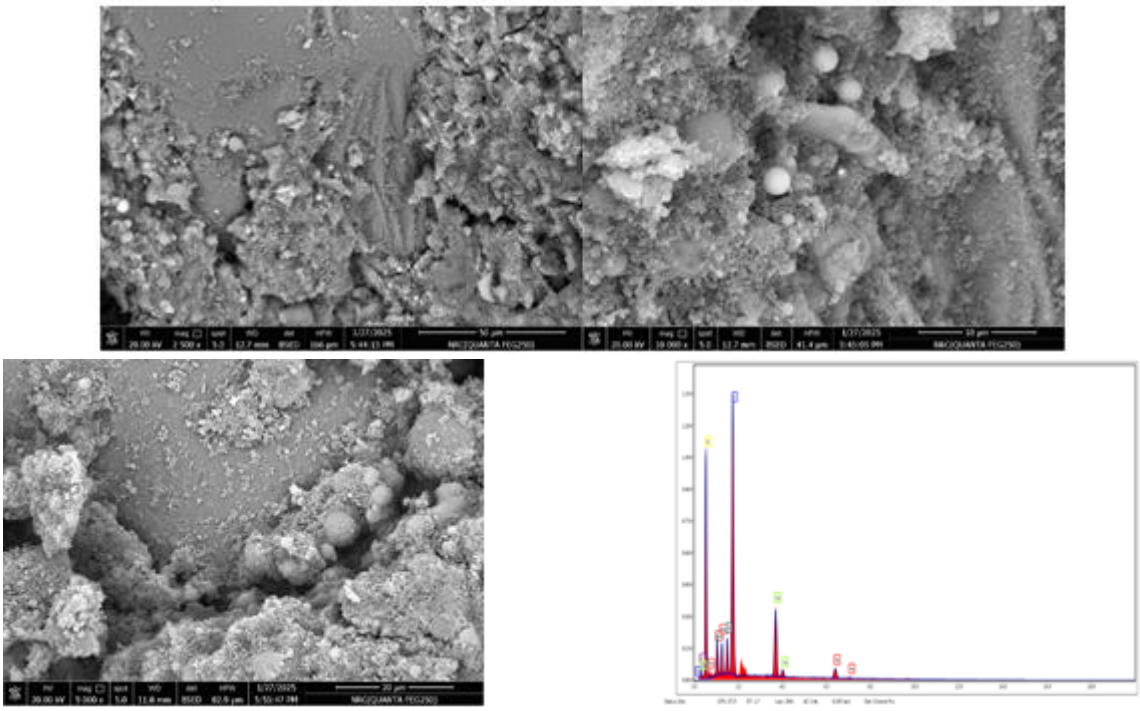

(b) NSF 0.25-A0.35

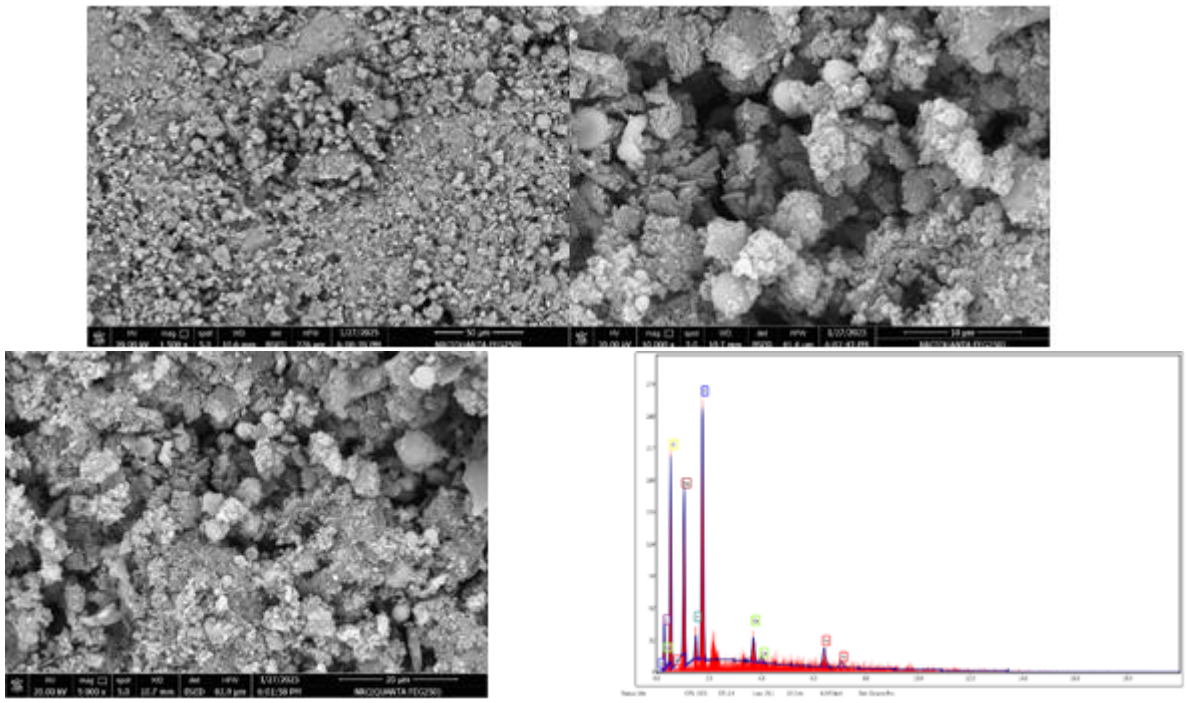

(c) SN2.0

Fig. 20: SEM Image and EDX spectrum analysis for FA-based GC samples

The geopolymer specimen without silicate fume (Figure 20.a) exhibited a relatively smooth matrix accompanied by the presence of large pores, microcracks, and partially reacted FA particles. In contrast, the NSF 0.25-A0.35 mix, activated using a 1:1 ratio of NaOH to silicate fume, displayed a significantly denser microstructure, as shown in Figure 20.b. According to Kang-Wei et al. [65], the presence of unreacted silica fume contributes to pore refinement by filling voids within the binder phase, thereby reducing overall porosity. Moreover, the incorporation of SF promoted the formation of additional gel phases,

contributing to a more compact microstructure and improved mechanical performance. Elemental analysis through EDX confirmed that silicon, aluminum, calcium, sodium, and iron were the predominant constituents in the geopolymer matrix. However, in the SN2.0 mix (Figure 20.c), which contained a NaOH-to-silicate fume ratio of 1:2, the microstructure appeared less cohesive. This may be attributed to the excessive silicate content, which, as reported in previous studies [56, 57], can hinder the geopolymerization process. Excessive soluble silicates may interfere with the formation of the geopolymeric gel network, thereby reducing the mechanical strength, as observed in sample SN2.0.

Microstructural analysis indicates that the incorporation of silica fume promotes densification and diminishes porosity, correlating with enhanced mechanical strength. In contrast, samples containing lower silica fume or modified sodium concentration demonstrate increased porosity or cracking in their microstructures, which may result in diminished performance. Elemental investigations corroborate these findings, indicating elevated Si and Al concentrations and advantageous Si/Al ratios linked to denser, more cohesive geopolymer matrices. The presence and ratios of calcium and sodium affect the formation of different binding phases, hence influencing durability and strength.

6. Conclusions

This study proposed a novel, sustainable method for formulating GC by employing SF in two capacities: as a partial replacement for FA and as a substitute for commercial Na_2SiO_3 in the activator solution. The incorporation of treated rubber fibers effectively fulfills the dual objectives of mechanical improvement and waste material valorization. Collectively, these developments significantly advance the creation of ambient-cured, high-performance geopolymer concretes that are environmentally sustainable and structurally proficient. This study yields the following findings based on the experimental results:

- The direct dissolution of SF in NaOH has demonstrated efficacy as a sustainable alternative to traditional Na_2SiO_3 as an activator. At a 25% SF replacement level, this innovative approach resulted in a significant improvement in the $f_{comp.}$ Of the GC mix.
- Increasing the substitution ratio of FA with SF resulted in diminished workability. At a 35% SF replacement level, fast setting and hardening were noted, requiring a gradual increase in superplasticizer dosage to sustain acceptable consistency.
- The utilization of type C FA as the principal binder in all GC mixtures facilitated strength enhancement under ambient curing conditions. Enhanced strength improvements were observed when FA was partially substituted with SF.
- The mechanical performance of GC is enhanced with higher alkaline solution-to-binder (AL/binder) ratios, achieving optimal strength at a ratio of 0.4.
- Strength increase was attained by augmenting the SF-to-NaOH ratio, with an optimal peak identified at a ratio of 1.5. Beyond this juncture, more increments yielded diminishing returns.
- At an SF/NaOH ratio of 1.5, compressive, tensile, and flexural strengths increased by 28.0%, 26.9%, and 29.8%, respectively, demonstrating a significant relationship between activator composition and mechanical performance.

- The addition of treated rubber fibers at a volume of up to 0.30% led to substantial enhancements in 28-day strengths: $f_{comp.}$ Increased by 25.7%, splitting tensile strength by 44.5%, and flexural strength by 47.8%.
- A 25% substitution of SF for FA resulted in a 12.6% decrease in the modulus of elasticity; however, the incorporation of 0.3% rubber fibers partially mitigated this effect, yielding a 10.8% gain in modulus compared to control specimens.
- The experimental elastic modulus of GC closely matched predictions from the Iravani model (within 11%), while OPC values were more aligned with ACI estimations, and rubberized GC exhibited superior conformity with AS 3600 standards.
- Microstructural analyses employing SEM and EDX demonstrated a significant presence of amorphous gel phases in SF-based GC matrices, corroborating the noted enhancements in mechanical performance.

7. Research limitation and recommendations for further studies

This study focused on providing valuable insights into the mechanical behavior of GC incorporating SF in both binder and activator solution; however, several limitations should be acknowledged, and directions for future research are proposed:

- The experiment predominantly concentrated on short-term mechanical properties. The long-term durability performance, including resistance to harsh climatic conditions, freeze-thaw cycles, and chloride infiltration, has not been well addressed and requires additional investigation.
- The fire resistance characteristics of silica fume-enhanced geopolymer concretes were not evaluated in this work. Future studies must encompass thorough fire performance assessments to ascertain their appropriateness for applications necessitating fire safety considerations.
- Microstructural investigations using SEM and EDX are essential for comprehending internal bonding mechanisms; nevertheless, such analyses were restricted to specific mixtures. A comprehensive microstructural investigation using all silica fume ratios is advised to clarify the impact of differing silica fume concentrations on the material's interior structure.
- The possible impact of various fiber kinds and doses on the mechanical and durability properties of SF-based GC was not investigated. Subsequent research should integrate these aspects to enhance composite performance.
- Future research should incorporate comprehensive elemental analysis.

Abbreviation

FA, Fly ash; GC, Geopolymer concrete; SF, Silica fume; AL, Alkaline activator solution; Na_2SiO_3, Sodium silicate; NaOH, sodium hydroxide; OPC, Ordinary Portland concrete; $f_{comp.}$, Compressive strength; f_{ten}, Tensile strength; f_{flex}; Flexural strength; E_c, Modulus of elasticity of concrete

References

[1] Davidovits, J., 1991. Geopolymer: inorganic polymer new materials. J. Therm. Anal. 37, 1633e1656.

[2] A. Rastogi and V. K. Paul, "A critical review of the potential for fly ash utilization in construction-specific applications in India," *Environ. Res. Eng. Manag.*, vol. 76, no. 2, pp. 65–75, 2020. https://erem.ktu.lt/index.php/erem/article/view/25166.

[3] C. Jangam, D. B. Pannaskar, and P. R. Pujari, "Review on Production and Utilization of Fly Ash: An Indian Perspective," Int. Educ. Res. J., vol. 10, no. 4, Apr. 2024. https://ierj.in/journal/index.php/ierj/article/view/3386ierj.in

[4] D. Das and P. K. Rout, "Synthesis, characterization and properties of fly ash-based geopolymer materials," J. Mater. Eng. Perform., vol. 30, pp. 3213–3231, 2021.

[5] Z. Zheng and P. Deng, "Mechanical and fracture properties of slag/steel slag-based geopolymer fully recycled aggregate concrete," *Constr. Build. Mater.* vol. 413, Art. no. 134533, Jan. 2024. doi:10.1016/j.conbuildmat.2023.134533. https://doi.org/10.1016/j.conbuildmat.2023.134533.

[6] M. Heshmat, I. Amer, F. Elgabbas, and M. A. Khalaf, "Effect of binder and activator composition on the characteristics of alkali-activated slag-based concrete," *Sci. Rep.*, vol. 14, Art. no. 13502, 2024. Doi: 10.1038/s41598-024-63214-5. https://doi.org/10.1038/s41598-024-63214-5.

[7] W. Huang and H. Wang, "Formulation development of metakaolin geopolymer with good workability for strength improvement and shrinkage reduction," *J. Cleaner Prod.*, vol. 434, Art. no. 140431, Jan. 2024. doi:10.1016/j.jclepro.2023.140431. https://doi.org/10.1016/j.jclepro.2023.140431.

[8] Z. Sun, Q. Tang, B. S. Xakalashe, X. Fan, M. Gan, X. Chen, Z. Ji, X. Huang, and B. Friedrich, "Mechanical and environmental characteristics of red mud geopolymers," *Constr. Build. Mater.* vol. 321, Art. no. 125564, Feb. 2022. doi:10.1016/j.conbuildmat.2021.125564. https://doi.org/10.1016/j.conbuildmat.2021.125564.

[9] S. Mabroum, A. Moukannaa, A. El Machi, Y. Taha, M. Benzaazoua, and R. Hakkou, "Mine wastes based geopolymers: A critical review," Cleaner Eng. Technol., vol. 1, Art. no. 100014, Dec. 2020. doi:10.1016/j.clet.2020.100014. https://doi.org/10.1016/j.clet.2020.100014.

[10] L. N. Assi, K. Carter, E. Deaver, and P. Ziehl, "Review of availability of source materials for geopolymer/sustainable concrete," J. Cleaner Prod., vol. 263, Art. no. 121477, 2020. doi:10.1016/j.jclepro.2020.121477. https://doi.org/10.1016/j.jclepro.2020.121477.

[11] M. Amran, S. Debbarma, and T. Ozbakkaloglu, "Fly ash-based eco-friendly geopolymer concrete: A critical review of the long-term durability properties," J. Cleaner Prod., vol. 263, Art. no. 121477, 2020. doi:10.1016/j.jclepro.2020.121477. https://doi.org/10.1016/j.jclepro.2020.121477.

[12] M. Niu, P. Zhang, J. Guo, and J. Wang, "Effect of municipal solid waste incineration fly ash on the mechanical properties and microstructure of geopolymer concrete," Gels, vol. 8, no. 6, Art. no. 341, 2022. Doi: 10.3390/gels8060341. https://doi.org/10.3390/gels8060341.

[13] P. Pavithra, M. S. Reddy, P. Dinakar, B. H. Rao, B. K. Satpathy, and A. N. Mohanty, "A mix design procedure for geopolymer concrete with fly ash," J. Cleaner Prod., vol. 133, pp. 117–125, 2016. doi:10.1016/j.jclepro.2016.05.044. https://doi.org/10.1016/j.jclepro.2016.05.044.

[14] Ismail Luhar & Salmabanu Luhar (2022), A Comprehensive Review on Fly Ash-Based Geopolymer, Journal of Composites Science 6(8):219.

[15] Amer Hassan, Mohammed Arif, Mohd Shariq, Effect of curing condition on the mechanical properties of fly ash-based geopolymer concrete, SN Applied Sciences, 1(12), 2019, DOI: 10.1007/s42452-019-1774-8.

[16] M. Verma, K. Upreti, P. Vats, S. Singh, P. Singh, N. Dev, D. K. Mishra, and B. Tiwari, "Experimental analysis of geopolymer concrete: a sustainable and economic concrete using the cost estimation model," Adv. Mater. Sci. Eng., vol. 2022, Art. No. 7488254, 16 pp., 2022. doi:10.1155/2022/7488254. https://doi.org/10.1155/2022/7488254.

[17] A. I. Abdullah, W. R. Abdallah, M. A. Pyram, M. A. Khalaf, M. A. M. Ali, and A. O. Bamousa, "Eco-sustainable use of industrial wastes as cement-partial alternate in concrete composition," Adv. Civ. Eng., to be published 2025.

[18] N. K. K. Lee and H. K. Lee, "Improved reactivity of fly ash–slag geopolymer by the addition of silica fume," Adv. Mater. Sci. Eng., vol. 2016, Art. No. 2192053, 2016. doi:10.1155/2016/2192053. https://doi.org/10.1155/2016/2192053.

[19] W. Yang, Y. Zhang, Q. Li, et al., "Recent advances in fly ash based geopolymers: Structures, activators, and durability aspects," ACS Omega, vol. 6, no. 7, pp. 4782–4800, 2021. doi:10.1021/acsomega.1c00582.

[20] P. Chindaprasirt, P. Paisitsrisawat, and U. Rattanasak, "Strength and resistance to sulfate and sulfuric acid of ground fluidized bed combustion fly ash–silica fume alkali-activated composite," Adv. Powder Technol., vol. 25, no. 3, pp. 1087–1095, 2014. doi:10.1016/j.apt.2014.02.007. https://doi.org/10.1016/j.apt.2014.02.007.

[21] N. K. Lee, G. H. An, K. T. Koh, and G. S. Ryu, "Improved reactivity of fly ash–slag geopolymer by the addition of silica fume," Adv. Mater. Sci. Eng., vol. 2016, Art. No. 2192053, 2016. doi:10.1155/2016/2192053. https://doi.org/10.1155/2016/2192053.

[22] Ö. Ergeshov, S. Örklemez, A. Ketema, et al., "Influence of silica fume on the mechanical and microstructural properties and life cycle assessment of fly ash based geopolymer mortar," Arab. J. Sci. Eng., vol. 50, no. 4, 2025.

[23] Adak, D.; Sarkar, M.; Mandal, S. Effect of nano-silica on strength and durability of fly ash-based [23] D. Adak, M. Sarkar, and S. Mandal, "Effect of nano-silica on strength and durability of fly ash–based geopolymer mortar," Constr. Build. Mater. vol. 70, pp. 453–459, 2014. doi:10.1016/j.conbuildmat.2014.07.093. https://doi.org/10.1016/j.conbuildmat.2014.07.093

[24] A. N. Sadiq, M. A. M. Ariffin, M. K. Anwar, H. S. Lee, and J. K. Singh, "Optimization and utilization of waste fly ash and silica fume based eco-friendly geopolymer mortar using response surface methodology," in Proc. 7th Malaysia–Japan Joint Int. Conf. 2022, IOP Conf. Ser.: Earth Environ. Sci., vol. 1144, Art. no. 012001, 2023. doi:10.1088/1755-1315/1144/1/012001.

[25] P. B. Vijaya, K. P. Arun, N. Anand, P. D. Arumairaj, T. Dhilip, and M. Sanath Kumar, "Experimental investigation on fresh and hardened properties of high-calcium fly ash based geopolymer concrete," Mater. Sci. Forum, vol. 1048, pp. 412–419, 2022. (Presented at ICMSMT 2021).

[26] G. M. Canfield, J. Eichler, K. Griffith, and J. D. Hearn, "The role of calcium in blended fly ash geopolymers," J. Mater. Sci., vol. 49, pp. 5922–5933, 2014. Doi: 10.1007/s10853-014-8230-x.

[27] "Geopolymer mortar incorporating high-calcium fly ash and silica fume," Arch. Civ. Eng., vol. 65, no. 1, 2019.

[28] P. Duan, C. Yan, and W. Zhou, "Compressive strength and microstructure of fly ash based geopolymer blended with silica fume under thermal cycle," Cem. Concr. Compos. vol. 78, pp. 108–119, 2017. doi:10.1016/j.cemconcomp.2017.01.009. https://doi.org/10.1016/j.cemconcomp.2017.01.009.

[29] B. Tempest, O. Sanusi, J. Gergely, V. Ogunro, and D. Weggel, "Compressive strength and embodied energy optimization of fly ash–based geopolymer concrete," presented at the World of Coal Ash Conference, Lexington, KY, and May 2009.

[30] X. GAO, Q. L. Yu, A. Lazaro, and H. J. H. Brouwers, "Evaluating an eco-olivine nanosilica as an alternative silica source in alkali-activated composites," J. Mater. Civ. Eng., vol. 30, no. 3, pp. 1–8, 2018. Doi: 10.1061/ (ASCE) MT.1943-5533.0002169. https://doi.org/10.1061/ (ASCE) MT.1943-5533.0002169.

[31] S. Yeluri and N. Yadav, "Mechanical properties of rubber aggregates based geopolymer concrete – A review," in Proc. IOP Conf. Ser.: Mater. Sci. Eng., vol. 989, International Virtual Conference on Emerging Research Trends in Structural Engineering, 2020.

[32] S. Abbas, A. Ahmed, A. Waheed, W. Abbass, M. Yousaf, S. Shaukat, H. Alabduljabbar, and Y. A. Awad, "Recycled untreated rubber waste for controlling the alkali–silica reaction in concrete," Materials, vol. 15, no. 10, Art. no. 3584, 2022. Doi: 10.3390/ma15103584. https://doi.org/10.3390/ma15103584.

[33] F. Jokar, M. Khorram, G. Karimi, and N. Hataf, "Experimental investigation of mechanical properties of crumbed rubber concrete containing natural zeolite," Constr. Build. Mater. vol. 208, pp. 2019.

[34] ASTM Committee C09, Standard Specification for Coal Fly Ash and Raw or Calcined Natural Pozzolan for Use in Concrete, ASTM C618-19, ASTM Int., West Conshohocken, PA, 2019.

[35] M. Mortar, N. Najm, and [Salem], "The influence of molarity activity on the green and mechanical properties of geopolymer concrete," Constr. Mater., vol. 5, no. 1, Art. no. 16, 2025. Doi: 10.3390/constrmater5010016. https://doi.org/10.3390/constrmater5010016.
[36] ASTM Committee C09, Standard Specification for Concrete Aggregates, ASTM C33-07, ASTM Int., West Conshohocken, PA, 2007.
[37] S. V. Patankar, S. S. Jamkar, and Y. M. Ghugal, "Effect of water-to-geopolymer binder ratio on the production of fly ash-based geopolymer concrete," Int. J. Adv. Technol. Civ. Eng., vol. 2, no. 1, 2013.
[38] BS EN 12390-3:2002 – "Testing hardened concrete — Compressive strength of test specimens
[39] ASTM Committee C09, Standard Test Method for Splitting Tensile Strength of Cylindrical Concrete Specimens, ASTM C496-90, ASTM Int., West Conshohocken, PA, 1990.
[40] ASTM Committee C09, Standard Test Method for Flexural Strength of Concrete Using Simple Beam with Third-Point Loading, ASTM C78-02, ASTM Int., West Conshohocken, PA, 2002.
[41] ASTM Committee C09, Standard Test Method for Static Modulus of Elasticity and Poisson's Ratio of Concrete in Compression, ASTM C469-02, ASTM Int., West Conshohocken, PA, 2002.
[42] P. Azarsa and R. Gupta, "Comparative study involving effect of curing regime on elastic modulus of geopolymer concrete," Buildings, vol. 10, no. 6, Art. no. 101, 2020. Doi: 10.3390/buildings10060101. https://doi.org/10.3390/buildings10060101.
[43] R. Manickavasagam and G. Mohan Kumar, "Short term properties of high-calcium fly ash based geopolymer binder," IOSR J. Mech. Civ. Eng., vol. 14, no. 1, pp. 13–20, Jan.–Feb. 2017.
[44] S. Thokchom, D. Dutta, and S. Ghosh, "Effect of incorporating silica fume in fly ash geopolymers," Int. J. Civ. Environ. Eng., vol. 5, no. 12, pp. 750–754, 2011.
[45] F. N. Okoye, J. Durgaprasad, and N. B. Singh, "Effect of silica fume on the mechanical properties of fly ash based geopolymer concrete," Ceram. Int., vol. 42, no. 2, pp. 3000–3006, Feb. 2016. doi:10.1016/j.ceramint.2015.10.084. https://doi.org/10.1016/j.ceramint.2015.10.084
[46] A. K. Mohapatra, D. K. Bera, and A. K. Rath, "Effect of silica fume on strength enhancement of geopolymer mortar in ambient curing," paper presented at the First Online Conference, 3 July 2020, pp. 819–830.
[47] H. Castillo, H. Collado, T. Droguett, S. Sánchez, M. Vesely, P. Garrido, and S. Palma, "Factors affecting the compressive strength of geopolymers: a review," Minerals, vol. 11, no. 12, Art. no. 1317, Dec. 2021. Doi: 10.3390/min11121317. https://doi.org/10.3390/min11121317.
[48] Z. Zuhua, X. Y., H. Z., and C. Yue, "Role of water in the synthesis of calcined kaolin based geopolymer," J. Clay Sci., 2008.
[49] D. Hadjito, S. E. Wallah, and B. V. Rangan, "Study on engineering properties of fly ash based geopolymer concrete," J. Austr. Ceram. Soc., vol. 38, pp. 44–47, 2002.
[50] S. A. Bernal, E. D. Rodríguez, R. M. de Gutiérrez, J. L. Provis, and S. Delvasto, "Activation of metakaolin/slag blends using alkaline solutions based on chemically modified silica fume and rice husk ash," Waste Biomass Valorization, vol. 3, pp. 99–108, 2012. Doi: 10.1007/s12649-011-9093-3. https://doi.org/10.1007/s12649-011-9093-3.
[51] J. E. Oh, P. J. M. Monteiro, S. S. Jun, S. Choi, and S. M. Clark, "The evolution of strength and crystalline phases for alkali-activated ground blast furnace slag and fly ash-based geopolymers," Cem. Concr. Res., vol. 40, pp. 189–196, 2010. doi:10.1016/j.cemconres.2009.10.003. https://doi.org/10.1016/j.cemconres.2009.10.003.
[52] T. Phoo-ngernkham, A. Maegawa, N. Mishima, S. Hatanaka, and P. Chindaprasirt, "Effects of sodium hydroxide and sodium silicate solutions on compressive and shear bond strengths of FA–GBFS geopolymer," Constr. Build. Mater. vol. 91, pp. 1–8, 2015. doi:10.1016/j.conbuildmat.2015.05.076. https://doi.org/10.1016/j.conbuildmat.2015.05.076.
[53] T. W. Cheng and J. P. Chiu, "Fire-resistant geopolymer produced by granulated blast furnace slag," Miner. Eng., vol. 16, no. 3, pp. 205–210, 2003. Doi: 10.1016/S0892-6875(03)00008-6. https://doi.org/10.1016/S0892-6875 (03)00008-6 scispace.com.
[54] H. Xu and J. S. J. van Deventer, "The geopolymerisation of alumino-silicate minerals," Int. J. Mineral Process., vol. 59, no. 3, pp. 247–266, 2000. Doi: 10.1016/S0301-7516(99)00074-5. https://doi.org/10.1016/S0301-7516(99)00074-5.

[55] B. Joseph and G. Mathew, "Influence of aggregate content on the behavior of fly ash based geopolymer concrete," Scientia Iranica, vol. 19, no. 5, pp. 1188–1194, 2012. doi:10.1016/j.scient.2012.07.006. https://doi.org/10.1016/j.scient.2012.07.006.

[56] E. S. S. Wardhono, R. Risdianto, and S. Sabariman, "The effect of sodium silicate to NaOH ratio on strength development of fly ash geopolymer mortar in marine environment," E3S Web Conf., vol. 445, Art. No. 01005, 2023. doi:10.1051/e3sconf/202344501005.

[57] B. Kumar, A. Kumar, and D. Singh, "Influence of sodium silicate to sodium hydroxide ratio on mechanical and microstructural properties of fly ash geopolymers," Materials Today: Proc., vol. 45, pp. 321–327, 2021. doi:10.1016/j.matpr.2021.02.338. https://doi.org/10.1016/j.matpr.2021.02.338.

[58] M. Olivia and H. Nikraz, "Properties of fly ash geopolymer concrete designed by Taguchi method," Materials and Design, vol. 36, pp. 191–198, 2012. doi:10.1016/j.matdes.2012.10.036. https://doi.org/10.1016/j.matdes.2012.10.036.

[59] D. Bondar, C. J. Lynsdale, N. B. Milestone, N. Hassani, and A. A. Ramezanianpour, "Engineering properties of alkali-activated natural pozzolan concrete," ACI Materials Journal, vol. 108, no. M08, pp. 64–72.

[60] C. Puttbach and S. M. Soroushian, "A detailed review of equations for estimating elastic modulus in specialty concretes," J. Mater. Civ. Eng., vol. 35, no. 6, 2023. doi:10.1061/JMCEE7.MTENG-14699. https://doi.org/10.1061/JMCEE7.MTENG-14699.

[61] ACI Committee 318, Building Code Requirements for Structural Concrete (ACI 318-19) and Commentary (ACI 318R-19), American Concrete Institute, Farmington Hills, MI, 2019, 520 pp.

[62] Standards Australia, AS 3600: Concrete Structures, Sydney, NSW: Standards Australia International Ltd, 2018.

[63] P. Nath and P. K. Sarker, "Flexural strength and elastic modulus of ambient-cured blended low-calcium fly ash geopolymer concrete," Constr. Build. Mater. vol. 130, pp. 22–31, Jan. 2017. doi:10.1016/j.conbuildmat.2016.11.034. https://doi.org/10.1016/j.conbuildmat.2016.11.034

[64] S. Iravani, "Mechanical properties of high-performance concrete," ACI Materials Journal, vol. 93, no. 5, pp. 416–426, Sept.–Oct. 1996.

[65] K.-W. Lee, K.-L. Lin, T.-W. Cheng, Y.-M. Chiu, and J.-L. Lee, "Evaluation of the mechanical and microstructural properties of eco-friendly alkali-activated slag concrete," Constr. Build. Mater. vol. 143, pp. 455–463, 2017. doi:10.1016/j.conbuildmat.2017.03.154.